PCCP

Accepted Manuscript

ROYAL SOCIETY OF CHEMISTRY

www.rsc.org/pccp

Cite this: DOI: 10.1039/c0xx00000x

www.rsc.org/xxxxxx

ARTICLE TYPE

Tip-Enhanced Raman Spectroscopic Measurement of Stress Change in Local domain of Epitaxial Graphene on the Carbon Face of 4H-SiC (000-1)

Toshiaki Suzuki,[1] Tamitake Itoh,[2*] Sanpon Vantasin,[1] Satoshi Minami,[1] Yasunori Kutsuma,[3] Koji Ashida,[3] Tada-aki Kaneko,[3] Yusuke Morisawa,[4] Takeshi Miura,[5] and Yukihiro Ozaki[1*]

Received (in XXX, XXX) Xth XXXXXXXXX 20XX, Accepted Xth XXXXXXXXX 20XX
DOI: 10.1039/b000000x

We improve bulk silver tip for tip-enhanced Raman scattering (TERS) and obtain TERS spectra of epitaxial graphene on the carbon face of 4H-SiC (000-1) with high signal-to-noise ratio. Thanks to the high quality of TERS spectra we firstly find out that the G band in the TERS spectra exhibits position-by-position variations in both lower wavenumber shifts and spectral broadening. The analysis of the variations reveals that the shifts and broadenings have a linear correlation each other, indicating that the variations are induced by the position dependent local stress on the graphene based on a uniaxial strain model.

Graphene has been the focus of a wide variety of research regarding its unique material properties, for example elasticity, charge carrier mobility, optical transparency, and chemical stability.[1-4] The character of graphene is changed by an interaction with a substrate and the distortion of local graphene structure. Thus, the interaction and distortion in a very small area should be explored to apply graphene to an electronic device. Raman spectroscopy is widely employed for investigating crystallinity of graphene.[5-8] In a Raman spectrum of graphene three representative signals named G, G', and D bands are observed at about 1600, 2700 and 1350 cm^{-1}, respectively. The G and G' bands are common for sp^2 carbon systems. The D band is due to defects in graphene, allowing us to investigate the structure of defects.

Raman spectra of graphene change with its structure, defect, and strain. The number of layers, structure, and defects of graphene has been explored using peak shifts, intensity variations, and changes band width.[7-12] Moreover, Raman imaging measurement allows visualizing local structure distribution of graphene.[13-15] However, spatial resolution of Raman scattering is restricted by the diffraction limit of light. Thus, the spectroscopic techniques realizing higher spatial resolution have recently been highly desired. The spatial resolution of tip-enhanced Raman scattering (TERS) is determined by the radius of a tip and can exceed the diffraction limit of light.[16,17] Signal enhancement in TERS, whose mechanism is intrinsically the same as that of surface enhanced Raman scattering[18], enables Raman spectral detection from such local areas. Thus, TERS has been a matter of keen interest in graphene research, and several research groups reported TERS studies of graphene.[19-22] Saito et al. measured TERS spectra of the edge boundary of exfoliated graphene fabricated on Si with the spatial resolution of 30 nm.[19] They studied position dependence of TERS spectra and found G band shifts due to excess charge effect and D band peak fluctuations due to the local strain distribution within the layers. More recently Wang et al. reported TERS measurement of exfoliated graphene by using a TERS probe consisting of gold nanoparticles.[20] They induced reversible artificial defects and control them by the TERS probe. However, TERS study of the exfoliated graphene has difficulty in controlling the graphene property due to mechanical distortion. Some groups reported TERS study of the graphene prepared by a silicon carbide (SiC) thermal decomposition method[21] and a chemical vacuum deposition (CVD) method[22] and discussed about TERS enhancement factors and edge structures. These methods can prepare homogeneous graphene with higher quality in larger area and have been expected to open a route for large-scale production of graphene-based devices.[23] The quality of the epitaxial graphene prepared by CVD and SiC thermal decomposition method depends on the local interaction between the substrate and graphene. However, TERS study of the local interaction has not been explored.

In the present study, we measured TERS spectra of epitaxial graphene on the carbon face of a SiC substrate developed by SiC thermal decomposition method, and analyzed the TERS spectra compared with conventional Raman spectra. By using the tip made of bulk silver, we obtained remarkably enhanced TERS spectra. The comparison between the TERS and Raman spectra reviled that the G bands in TERS spectra show lower wavenumber shifts and their band widths become broad significantly. These band shifts and broadenings exhibit position dependences, and there is clear correlation between the band shifts and the broadenings. On the basis of a uniaxial strain model of graphene,[24] we clarified that these spectral variations reflect local strain in graphene from the SiC substrate.

Method and materials

The epitaxial graphene was prepared by the method of suppressing the Si sublimation from the carbon-face (C-face) of SiC. A tantalum carbide (TaC) semi-closed container was

employed to demonstrate 1800 ºC confinement growth of C-face graphene. The graphene was grown at 1800 ºC for 1 min in the TaC container. The vapor phase inside was composed of the evaporated vapor species from the SiC substrate. Precise control of the Si pressure was obtained by changing the vacuum of the container. An etching reaction under Si pressure conditions took place, resulting in the suppression of the thickness of graphene layer. The averaged number of graphene layers estimated by optical absorption spectroscopy was 1.7 layers.

Raman and TERS spectra were measured by an instrument consisting of a reflection-mode Raman microscope and an AFM instrument (Photon Design, Nanostar NFRSM800). This system was arranged to introduce excitation light from the top of the sample and to collect backscattered signals using a 90× objective lens (numerical aperture, NA = 0.71). The 514.5 nm line from an Argon laser (Spectra Physics, Stabilite 2017-06S) was used as the excitation light. The laser power of TERS experiment at the sample point was 100 μw. A bulk silver needle prepared in cooperation with UNISOKU Co. LTD by an electrochemical etching method was used as the TERS tip needle, which was attached to a quartz tuning fork of a shear-force-based AFM at an angle of 45º. The tip radius of the probe was about 75 nm. The TERS tip approached the sample using the non-contact mode. A Raman signal was first collected under the tip-retracted conditions, and then, under the tip-approaching conditions at the same point. A TERS spectrum was obtained by subtracting the spectrum observed under the tip-retracted conditions from that collected under the tip-approaching conditions. Raman spectra observed under the tip-retracted condition were used as normal Raman spectra.

Result and Discussion

Figure 1b shows a Raman spectrum in the 4500-1000 cm^{-1} region at a particular spot in epitaxial graphene on the 4H-SiC (000-1) surface measured under tip-retracted conditions. Thus, it is a normal Raman spectrum. In this spectrum, Raman signals due to G and G' modes are observed at 1592 and 2703 cm^{-1}, respectively. Many signals arising from the SiC substrate can be seen in the 1900-1200 cm^{-1} region. Figure 1a shows a spectrum obtained under tip-approaching conditions. One can easily see that a number of Raman signals are enhanced when the tip approaches to the sample. Particularly, signals at 2695 and 1584 cm^{-1} are enhanced strongly. Moreover, signals at 3246 and 2450 cm^{-1} become strong markedly, and those at 4282 and 2928 cm^{-1}, which do not appear or are almost missing in Fig. 1b, appear clearly in Fig. 1a. The signals at 3246, 2928, and 2450 cm^{-1} may be assigned to G"(2LO), G＋D、G*(LA+iTO), respectively.[25] The assignment of the 4282 cm^{-1} peak has been unknown. The position, shape, and intensity of this peak looks similar to G+G' peak, which is reported by Rao et al. at 4250 cm^{-1}, using 2.33 eV laser.[24] They also indicates that G+G' peak shifts to higher frequency with higher photon energy (100 cm^{-1}/eV).[25] From Ref. 25, we can calculate that G+G' peak appear at 4258 cm^{-1} because we used 2.41 eV laser. Thus, we tentatively attribute the observed peak at 4282 cm^{-1} to G+G' mode.

The spectrum in Fig. 1c was obtained by subtracting the spectrum in Fig. 1b from that in Fig. 1a. Thus, Figure 1c depicts a TERS spectrum of epitaxial graphene on the 4H-SiC (000-1) surface excluding the normal Raman spectrum. Of note in the TERS spectrum is that the signal-to-noise ratio is extremely high. This demonstrates the superiority of the developed silver TERS tip probe. The G' band in the TERS spectrum (Fig. 1a) is enhanced by 640 % compared with the normal Raman spectrum (Fig. 1b). The enhancement factor of the TERS spectrum in Fig. 1 is superior to those of any TERS spectra of graphene previously reported.[21] This may be the first time that the 4282 cm^{-1} peak (G+G' peak) has ever been observed in a TERS spectrum of graphene. The enhancement factor of the TERS can be estimated using the ration between area for near-field Raman detection and that for far-field one of 1/180 and signal total signal enhancement of 640 % to be about 1000. We added three tyapical SEM imeges of TERS active tips showing strong, normal, and weak TERS signals in Fig. S1. The SEM images indicates that small curvatures of tip tops is important to contribute to achieve the large enhancement factors.

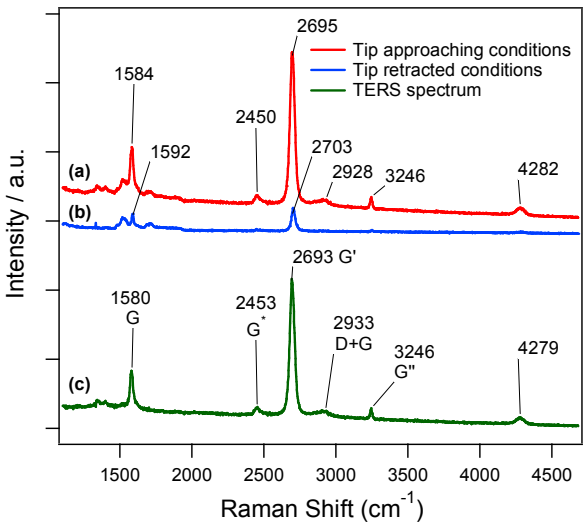

Fig. 1 Raman spectra of epitaxial graphene on the carbon surface of the 4H-SiC (000-1) measured under (a) tip-approaching conditions, and (b) tip-retracted conditions. (c) The difference spectrum calculated by subtracting the spectrum (b) from the spectrum (a). (TERS spectrum)

Although the signals due to the graphene are enhanced strongly, those in the 1700-1200 cm^{-1} region from the SiC substrate are little enhanced. In this way one can selectively observe the signals from the graphene on the C-face of the SiC substrate by using TERS. These results are different from those by Domke et al.[21] They used graphene grown on the Si-face of SiC, not C-face. The mechanism of graphene growth on the Si-face is different from that on the C-face. Thus the property of an interfacial layer of each type of graphene is different to each other. Therefore, TERS spectra may be different between the C- and Si-face.

In Fig. 1, the intensity ratio of G'-band and G-band in the TERS spectrum (Fig. 1c) seems to be smaller than that in the normal Raman spectrum (Fig. 1b). The intensity ratios of G'-band and G-band increase by increasing in the number of layers[5]. Thus, the smaller intensity ratios for the TERS spectrum in Figs. 1b and 1c indicates that the number of layers at the TERS detection area is smaller than the averaged number of layers at the conforcal Raman detection area. Another posibility is

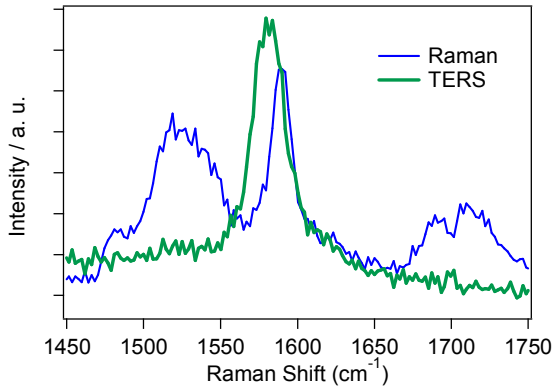

Fig. 2 Enlarged Raman and TERS spectra in the 1750-1450 cm^{-1} region of epitaxial graphene on the carbon surface of the 4H-SiC (000-1) from Fig. 1.

concentration of defects, because the defects in graphene surfaces decreases the intensity ratios.[8] Thus, the concentration of defect at the TERS detection area may be smaller than that at at the conforcal Raman detection area. The large enhancement factors of the current TERS tip enable us such detailed discussion of TERS spectra.

Note that the G band of the TERS spectrum shows a lower wavenumber shift by 12 cm^{-1} from that of the Raman spectrum (see Fig. 1b and Fig. 1c). Figure 2 depicts the enlarged spectra in the G band region (the 1750-1450 cm^{-1} region) for the Raman and TERS spectra in Fig. 1. The comparison of the G band in the TERS spectrum with that in the Raman spectrum shows not only the band shift but also a change in the band width. From curve fitting, the full width at half maximum (FWHM) changes from 14 cm^{-1} to 24 cm^{-1} upon going from the Raman spectrum to the TERS spectrum. It is very likely that the large change in the band width occurs due to the fact that the spatial resolution of TERS is much higher than that of normal Raman scattering, and TERS observes much smaller area. The spatial resolution of our Raman microscope is 1 μm. Thus, the Raman spectrum collects averaged signals from a measured area. On the other hand, the special resolution of the TERS spectrum is approximately determined by radius of the tip.[26] In the present case, it is 75 nm, and thus the spatial resolution of the TERS spectrum is 75 nm. Thus, the differences between the TERS and Raman spectra may arise from changes in fine structure and local conditions. Note that the G band width for TERS is broader than that for normal Raman, indicating the result is not due to common inhomogeneous

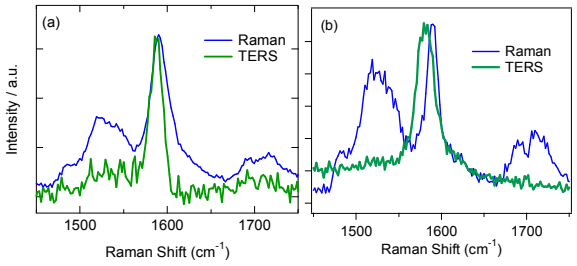

Fig. 3 TERS and Raman spectra of the graphene measured at different points (a-c), and the plot of a correlation between the peak shift and the ⊿FWHM of the G band at different positions (d). The S/N ratio is worth in TERS than the Raman spectrum for (a). The reason for the S/N ratio low for the TERS is un-optimized TERS detection.

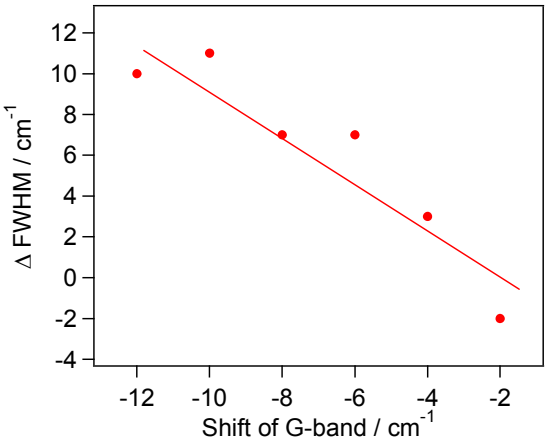

Fig. 4 The plot of a correlation between the peak shift and the ⊿FWHM of the G band at different positions (d).

broadening, but due to some local properties which is negligible for normal Raman.

We measured TERS spectra of graphene by changing positions, and found that the peak shift of the G band and the change of its FWHM are different from place to place as shown in Fig. 3a and 3b. We evaluated the relationship between variations in the peak shifts and those in FWHMs using the normal Raman spectra as standard spectra independent of TERS spectral variations. Figure 4 plots the difference in G-band width between the normal Raman and the TERS spectra (⊿FWHM) versus the peak shift of G-band. There is correlation between the peak shifts and the ⊿FWHMs. As the absolute value of peak shift of the G band becomes larger in the TERS spectrum, its ⊿FWHM increases. Note that the spectral variations in normal Raman spectra are excluding from Fig. 4 by subtracting signals at tip approaching from signals at tip retracting as shown in Fig. 1.

It has been known from Raman studies of graphene that the G band shift and broadening are mainly induced by two kinds of perturbations; hole and electron doping[27, 28] and stress on the graphene.[24] We here discuss which perturbation occurred the G band shifts and broadening. G band shifts and changes in the FWHM have been observed by doping hole and electron with applying the voltage to graphene.[27, 28] In the current TERS measurement, however, no voltage is applied to the sample. Also the electrical interaction between the graphene on the C-face and the substrate is weak, and thus its effect on the G band may be small. Furthermore the effects of static charges on the tip or/and sample surfaces are negligible because evidence of static charges, which is distortion of AFM images (see Fig. 5) and instability in tips approach, did not observed in the current experiment. Thus, we excluded the first possibility and focus ourselves on the stress on graphene as the origin of the G band shifts and broadening.

Then we here discuss the origin of the stress. In the SiC thermal decomposition method, the graphene is fabricated through thermal procedure. Coefficient of thermal expansion of graphene layer (-9×10^{-6} K^{-1})[29] is different from that of the SiC substrate (4×10^{-6} K^{-1})[30], inducing the difference generates thermal stress between the SiC and the graphene during a cooling process of the graphene just after its fabrication. Indeed when unidirectional stress is applied mechanically to graphene, the G band is split into two directions where the stress is applied and not applied, yielding the G^+ and G^- bands.[24] When the stress is

weak, the splitting of G band is small and looks broadening. It has also been reported that the G band shows a lower wavenumber shift by applying the stress to graphene because of distortion of the graphene lattice.[31] In the current preparation conditions of graphene, ridge structures are commonly observed in AFM images as shown in Fig. 5. The graphene at the ridge part is somewhat away from the substrate, and thus distortion of the graphene lattice is significantly different from that at the flat part. As shown in Fig. 5, the graphene surface has a wide flat area (about several μm) and a very small ridge structure area. In the normal Raman spectra, the signal from the flat area is dominant. On the other hand, the signal from the ridge structure can also be observed in the TERS spectra, because the spatial resolution of TERS is much higher than that of normal Raman. Thus, we consider that variations in the local stress at ridge structures are the origin of the observed variations in G band.

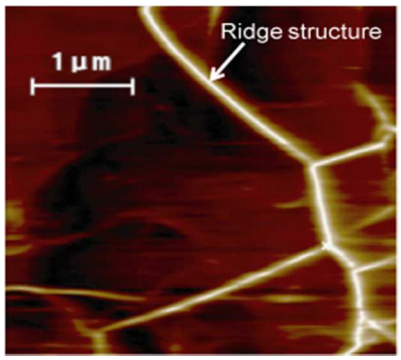

Fig. 5. AFM topographic image of the graphene on C-face of 4H-SiC (000-1).

We here compare our consideration with previous reports. In Ref. 19, Saito et al attribute G band shifts to the excess charge effect on graphene. They used exfoliated graphene films on glass plates, which work as insulators for excess charge. Thus, it is reasonable that excess charge remains on the plates and may induce G band shifts. However, in our work we used epitaxial graphene on the carbon face. Thus, the excess charge effect on graphene is negligible because of electrical conductivity of carbon face. It was reported that a force applied by a tip change the G band of carbon nanotube to a lower wavenumber regions.[32] However, the present TERS experiment was carried out under a non-contact mode, and thus, the effect of the force from the tip seems to be much smaller than that in the experiment by Yano et al., who used a contact mode.[32] In the current case the degree of the G band shift and broadening shows position-by-position variations. Therefore, the variations are likely induced by the position-dependent stress at the ridge structures generated during the fabrication of epitaxial graphene on the C-face.

Additionally we discuss the variations of peak shift and FWHM in the normal Raman spectra. In Figs. 2 and 3, the variations are also dependent upon positions, i.e. FWHM of the normal spectrum (Fig. 3a) is larger than that in (Fig. 3b). We consider that the variations in peak shift and FWHM of G bands are due to stress macroscopically induced by distortion of graphene surfaces during the preparation of grapheme. [24]

Conclusions

In this work, we measured TERS spectra of epitaxial graphene on the carbon face of 4H-SiC (000-1) and compared them with the corresponding normal Raman spectra. Thanks to the high enhancement factor of the developed bulk silver tip, it was clearly found that the G band in the TERS spectra exhibits position-by-position variations in the lower wavenumber shift and the spectral broadening, and we have concluded that these spectral changes occur by the position-dependent variation of stress on the C-face of 4H-SiC(000-1).

Now we are trying many TERS line measurements to obtain the relationship between ridge structures and G bands, but thermal drift of samples has prevented us from the correct line detections using both AFM and TERS imaging. Figure S2 is a rear case of successful line detection. To resolve the thermal drift, we are now developing a TERS system with a cooling sample room in a vacuum chamber. Such system is important for not only the understanding, prediction, and control of graphene electronic dynamics by TERS tips but also the development of electromagnetic strong coupling systems composed of molecular systems and plasmonic ones using quantum electrodynamics.[33,34] Such systems may provide new insights into the coupling among electrons, excitons, plasmons, and photons for graphene technology.

Acknowledgment

This work was supported by JST on A-STEP Grant Number AS2525017J and in part by JSPS KAKENHI Grant-in-Aid for Scientific Research (C) Number 20510111 and (B) Number 26286066.

Notes and references

[1] *Department of Chemistry, School of Science and Technology, Kwansei Gakuin University, Gakuen 2-1, Sanda, Hyogo 669-1337, Japan. Fax: +81-795-65-9077; Tel: +81-795-65-8349 Email: ozaki@kwansei.ac.jp*
[2] *Nano-Bioanalysis Research Group, Health Research Institute, National Institute of Advanced Industrial Science and Technology (AIST), Takamatsu, Kagawa 761-0395, Japan. Fax: +81-87-869-4113; Tel: +81-87-869-3557; E-mail: tamitake-itou@aist.go.jp*
[3] *Department of Physics, School of Science and Technology, Kwansei Gakuin University, Gakuen 2-1, Sanda, Hyogo 669-1337, Japan.*
[4] *Department of Chemistry, School of Science and Engineering, Kinki University, 3-4-1 Kowakae, Higashi-Osaka, Osaka 577-8502, Japan.*
[5] *UNISOKU Co. Ltd., 2-4-3 Kasugano, Hirakata, Osaka 573-0131, Japan.*

1 C. Lee, X. D. Wei, J. W. Kysar, and J. Hone, *Science, 2008,* **321**, 385-388.
2 A. K. Geim, *Science,* 2009, **324**, 1530-1534.
3 K. P. Loh, Q. L. Bao, P. K. Ang, and J. X. Yang, *J. Mater. Chem.,* 2010, **20**, 2277-2289.
4 S. Bae, H. Kim, Y. Lee, X. F. Xu, J. S. Park, Y. Zheng, J. Balakrishnan, T. Lei, H. R. Kim, Y. I. Song, Y. J. Kim, K. S. Kim, B. Ozyilmaz, J. H. Ahn, B. H. Hong, and S. Iijima, *Nat. Nanotechnol.,* 2010, **5**, 574-578.
5 L. M. Malard, M. A. Pimenta, G. Dresselhaus, and M. S. Dresselhaus, *Phys. Rep.,* 2009, **473**, 51-87.
6 R. Saito, M. Hofmann, G. Dresselhaus, A. Jorio, and M. S. Dresselhaus, *Adv. Phys.,* 2011, **60**, 413-550.
7 A. Jorio, M. Dresselhaus, R. Saito, and G. F. Dresselhaus, *Raman Spectroscopy in Graphene related systems* Wiley-VCH, Weinheim (2011).
8 J.Stadler, T. Schmid and R. Zenobi, ACS Nano 5 , (2011), 8442-8448.

9 C. Casiraghi, S. Pisana, K. S. Novoselov, A. K. Geim, and A. C. Ferrari, *Appl. Phys. Lett.,* 2007, **91**, 233108.

10 J. Yan, Y. B. Zhang, P. Kim, and A. Pinczuk, *Phys. Rev. Lett.,* 2007, **98**, 166802.

11 S. Pisana, M. Lazzeri, C. Casiraghi, K. S. Novoselov, A. K. Geim, A. C. Ferrari, and F. Mauri, *Nat. Mater,* 2007, **6**, 198-201.

12 D. Graf, F. Molitor, K. Ensslin, C. Stampfer, A. Jungen, C. Hierold, and L. Wirtz, *Nano Lett.,* 2007, **7**, 238-242.

13 S. Kataria, A. Patsha, S. Dhara, A. K. Tyagi, and H. C. Barshilia, *J. Raman Spectrosc.,* 2012, **43**, 1864-1867.

14 O. Ryong-Sok, A. Iwamoto, Y. Nishi, Y. Funase, T. Yuasa, T. Tomita, M. Nagase, H. Hibino, and H. Yamaguchi, *Jpn. J. Appl. Phys.,* 2012, **51**, 06FD06.

15 C. Stampfer, F. Molitor, D. Graf, K. Ensslin, A. Jungen, C. Hierold, and L. Wirtz, *Appl. Phys. Lett.,* 2007, **91**, 241907.

16 K. F. Domke, and B. Pettinger, *Chemphyschem,* 2010, **11**, 1365-1373.

17 P. Verma, T. Ichimura, T. Yano, Y. Saito, and S. Kawata, *Laser & Photonics Rev.,* 2010, **4**, 548-561.

18 K. Yoshida, T. Itoh, H. Tamaru, V. Biju, M. Ishikawa, Y. Ozaki, *Phys. Rev. B,* 2010, **81,** 115406; T. Itoh, M. Iga, H. Tamaru, K. Yoshida, V. Biju, and M. Ishikawa, *J. Chem. Phys.,* 2012, **136,** 024703.

19 Y. Saito, P. Verma, K. Masui, Y. Inouye, and S. Kawata, *J. Raman Spectrosc.,* 2009, **40**, 1434-1440.

20 P. J. Wang, D. Zhang, L. L. Li, Z. P. Li, L. S. Zhang, and Y. Fang, *Plasmonics,* 2012, **7,** 555-561.

21 K. F. Domke, and B. Pettinger, *J. Raman Spectrosc.,* 2009, **40**, 1427-1433.

22 M. Ghislandi, G. G. Hoffmann, E. Tkalya, L. J. Xue, and G. De With, *Appl. Spectrosc. Rev.,* 2012, **47**, 371-381.

23 H. Hibino, H. Kageshima, and M. Nagase, *J. Phys. D: Appl. Phys.,* 2010, **43**, 374005.

24 T. M. G. Mohiuddin, A. Lombardo, R. R. Nair, A. Bonetti, G. Savini R. Jalil, N. Bonini, D. M. Basko, C. Galiotis, N. Marzari, K. S. Novoselov, A. K. Geim, and A. C. Ferrari, *Phys. Rev. B,* 2009, **79**, 205433.

25 R. Rao, D. Tishler, J. Katoch, and M. Ishigami, *Phys. Rev. B,* 2011, **84**, 113406.

26 C. Höppener, Z. J. Lapin, P. Bharadwaj, and L. Novotny, *Phys. Rev. lett.,* 2012, **109**, 017402.

27 A. Das, S. Pisana, B. Chakraborty, S. Piscanec, S. K. Saha, U. V. Waghmare, K. S. Novoselov, H. R. Krishnamurthy, A. K. Geim, A. C. Ferrari, and A. K. Sood, *Nat. Nanotechnol.,* 2008, **3**, 210-215.

28 J. Yan, Y. Zhang, P. Kim, and A. Pinczuk, *Phys. Rev. Lett.,* 2007, **98**, 166802.

29 W. Z. Bao et al., *Nat. Nanotechnol.,* 2009, **4**, 562.

30 Harris, G. L. Properties of silicon carbide. IET. 1995, p. 19; 170–180.

31 M. A. Bissett, W. Izumida, R. Saito, and H. Ago, *ACS Nano,* 2012, **6**, 10229-10238.

32 T. Yano, P. Verma, Y. Saito, T. Ichimura, and S. Kawata, *Nat. Photonics,* 2009, **3**, 473-477.

33 T. Itoh, Y.S. Yamamoto, H. Tamaru, V. Biju, N. Murase, Y. Ozaki, *Phys. Rev. B,* 2013, **87**, 235408.

34 T. Itoh, Y.S. Yamamoto, H. Tamaru, V. Biju, S. Wakida, Y. Ozaki, *Phys. Rev. B,* 2014, **89**, 195436.

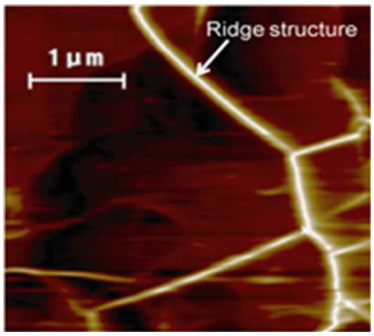

We measured TERS spectra of epitaxial graphene on the carbon face of 4H-SiC (000-1) and compared them with the corresponding normal Raman spectra.